

Measurement-device-independent quantum key distribution based on Bell's inequality

Hua-Lei Yin,^{1,2} Yao Fu,^{1,2} Yan-Lin Tang,^{1,2} Yuan Li,^{1,2} Teng-Yun Chen,^{1,2} and Zeng-Bing Chen^{1,2}

¹*Hefei National Laboratory for Physical Sciences at Microscale and Department of Modern Physics,
University of Science and Technology of China, Hefei, Anhui 230026, China*

²*CAS Center for Excellence and Synergetic Innovation Center of Quantum Information and Quantum Physics,
University of Science and Technology of China, Hefei, Anhui 230026, China*

We propose two quantum key distribution (QKD) protocols based on Bell's inequality, which can be considered as modified time-reversed E91 protocol. Similar to the measurement-device-independent quantum key distribution (MDI-QKD) protocol, the first scheme requires the assumption that Alice and Bob perfectly characterize the encoded quantum states. However, our second protocol does not require this assumption, which can defeat more known and unknown source-side attacks compared with the MDI-QKD. The two protocols are naturally immune to all hacking attacks with respect to detections. Therefore, the security of the two protocols can be proven based on the violation of Bell's inequality with measurement data under fair-sampling assumption. In our simulation, the results of both protocols show that long-distance quantum key distribution over 200 km remains secure with conventional lasers in the asymptotic-data case. We present a new technique to estimate the Bell's inequality violation, which can also be applied to other fields of quantum information processing.

PACS numbers: 03.67.Dd, 03.67.Hk, 03.67.Ac

I. INTRODUCTION

Quantum key distribution (QKD), such as BB84 [1] and E91 [2], provides a secure way to exchange private information. It enables a common string of random bits, called secret keys, to be shared secretly between the two legitimate users (typically called Alice and Bob). In principle, QKD exploits the fundamental laws of quantum mechanics to offer information-theoretical security [3, 4]. However, the gap between the ideal devices fulfilling the assumptions of security proof and the realistic ones opens various loopholes which make the system suffered from various kinds of side-channel attacks [5–9].

In general, there are two approaches to circumvent the side-channel attacks. The first one is trying to characterize realistic devices completely in the security proofs. This approach is quite difficult since it is almost impossible to have a special model that includes all practically relevant imperfections of realistic devices. The second one is known as (full) device-independent QKD (DI-QKD) [10, 11] whose security proof is based on the observation of nonlocal statistical correlations (loophole-free test of Bell's inequality) only and as such, it does not require detailed knowledge of the devices. A recent DI-QKD protocol has been proposed [12], where the violation of loophole-free Bell's inequality is not affected by the channel losses between Alice and Bob, because it only requires Bell test performed locally in Alice's site. Unfortunately, DI-QKD is currently highly impractical, for the reason that it requires the legitimate users to carry out a (full) loophole-free Bell test (very high detection efficiency and space-like separation between Alice and Bob), which is still a big experimental challenge even with the state-of-the-art technologies [13, 14]. More importantly, its secure key rate is very limited at practical distances even using the novel techniques, i.e., local Bell test [12]

or heralded qubit amplifier [15].

Recent progress has been made by introducing the novel idea of measurement-device-independent QKD (MDI-QKD) protocol [16], which is built on the idea of the time-reversed Einstein-Podolsky-Rosen protocol for QKD [17, 18]. The measurement devices in MDI-QKD, which can be treated as a true black box, are essentially used to post-select entanglement states from the mixed states between Alice and Bob. Thus, MDI-QKD closes all kinds of detection-side loopholes. Furthermore, one crucial advantage of the MDI-QKD is that the encoded quantum states can use weak coherent pulses (WCPs) combined with the decoy-state techniques [19–21] instead of single-photon sources. Besides, the secure key rate and transmission distance are comparable to that of usual QKD protocols with entangled sources [22, 23]. An important assumption in MDI-QKD is that Alice and Bob need to perfectly characterize the encoded quantum states. The secret key distribution of BB84 protocol is based on information encoded complementary bases, while the secret key distribution of E91 is based on quantum entanglement. The E91 protocol is the first QKD scheme whose security proof exploits the violation of Bell's inequality. As a security assumption of usual QKD, Alice and Bob need to trust their devices (both source-side and detection-side), the Bell test can then be performed with the measurement data under the fair-sampling assumption.

In this paper, we propose two QKD protocols based on Bell's inequality, which can be regarded as the modified time-reversed E91 protocol, denoted by P1 and P2. The two protocols are naturally immune to all possible detection-side attacks. P1 requires the assumption that Alice and Bob need to perfectly characterize the encoded quantum states. However, P2 does not require this assumption. Therefore, P2 is more device-independent,

which enables the system to defeat more known and unknown source-side attacks compared with the MDI-QKD. In contrast to DI-QKD, the two schemes proposed here do not require the legitimate users to perform a loophole-free Bell test. It is enough to prove our two schemes' security based on the violation of Bell's inequality with measurement data under fair-sampling assumption. We demonstrate that P1 is equivalent to the MDI-QKD protocol in the asymptotic case. Combining the conventional laser sources with vacuum+decoy+signal method, we simulate the secure key rates in the asymptotic-data case and the finite-data case, respectively. The results of both protocols show that long-distance quantum key distribution over 200 km remains secure with conventional lasers in the asymptotic-data case. We present a new technique to estimate the violation of Bell's inequality (the "Bell value"), which can be used to test local realism without preparing entanglement states in advance.

II. NECESSARY ASSUMPTIONS

For each QKD protocol, the security assumptions play a crucial role. In order to show our QKD protocols sufficiently, we first illustrate five fundamental assumptions of P1 and P2, which are also necessary in DI-QKD protocol [11, 12].

First, Alice and Bob's physical locations are isolated and secure, i.e., no unwanted information can leak out from the secure location. Second, they trust their quantum random number generators to generate a random output. Third, they can compute and store the classical data with their trusted classical devices. Fourth, the two legitimate users could share an authenticated classical channel. Fifth, the (quantum) devices of different users are causally independent. The last assumption is guaranteed when the devices' memory is totally erased after each process or the devices have no internal memory at all (this assumption is necessary for defeating memory attack [24]).

In addition to the above assumptions, the security of P1 and MDI-QKD will be guaranteed with another two assumptions. The first one is that the Hilbert space of quantum state preparation is two-dimensional. The second assumption is that Alice and Bob can perfectly characterize their encoded quantum states (e.g., the polarization encoded scheme of phase-randomized WCPs). Nevertheless, without the second security assumption, P2 still satisfy the security proof. Thus, P2 can defeat more known and unknown source-side attacks.

Note that it is also not required Alice and Bob to characterize their encoded quantum states perfectly in recent works [25–27], but the single-photon sources assumption is necessary. In our scheme, we use conventional laser sources (WCPs) which make our QKD protocols more practical and economical under current technology instead of single-photon sources.

III. PROTOCOL DESCRIPTION

In the following, we describe the QKD schemes in details, see Fig. 1. Alice and Bob independently and ran-

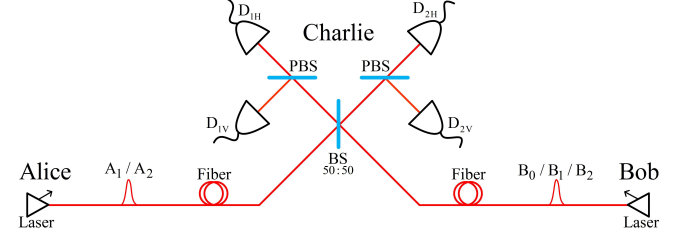


FIG. 1: (Color online) Basic setup of P1 and P2 protocols. For simplicity, we consider the polarization encoding scheme. Alice (Bob) randomly prepares two (three) settings $\{A_1, A_2\}$ ($\{B_0, B_1, B_2\}$) of quantum states with phase randomized WCPs. Charlie performs Bell state measurement and the measurement results are publicly announced. A successful Bell state measurement corresponds to the observation of only two of four detectors being clicked. $|\psi^+\rangle = 1/\sqrt{2}(|HV\rangle + |VH\rangle)$ represents a click in D_{1H} and D_{1V} , or D_{2H} and D_{2V} , while $|\psi^-\rangle = 1/\sqrt{2}(|HV\rangle - |VH\rangle)$ represents a click in D_{1H} and D_{2V} , or D_{2H} and D_{1V} .

domly prepare quantum states with phase randomized WCPs in two settings $\{A_1 = \sigma_z, A_2 = \sigma_x\}$ and three settings $\{B_0 = \sigma_z, B_1 = (\sigma_z + \sigma_x)/\sqrt{2}, B_2 = (\sigma_z - \sigma_x)/\sqrt{2}\}$, respectively. Then they send each pulse to an untrusted third party Charlie, who can be anybody, even the eavesdropper Eve. Charlie carries out a partial Bell state measurement (BSM). As is known, we cannot completely distinguish four Bell states simultaneously through singly using linear optical element. In this paper we can only unambiguously distinguish two Bell states $\{|\psi^+\rangle, |\psi^-\rangle\}$ (Fortunately, the identification of one Bell state is adequate to prove security). Charlie announces through a public channel whether he has received a Bell state and which Bell state he has received. Alice and Bob keep the raw data of successful BSM results and discard the rest. The Bell value can be estimated from the raw data of quantum states sent by Alice's and Bob's two settings (bases) $\{A_1, A_2\}$ and $\{B_1, B_2\}$, respectively. They post-select the results as a raw key when Alice and Bob choose setting A_1 and B_0 , respectively (here, $A_1 = B_0 = \sigma_z$). Decoy-state techniques are employed [19–21] to estimate the yield, bit error rate and Bell value, given that both Alice and Bob send out single-photon states (untagged portion). One party needs to carry out a bit flip to his or her raw data to guarantee that their raw key is correctly correlated. Then they perform error-correction and privacy amplification with one-way classical postprocessing to extract secure keys.

IV. SECURITY ANALYSIS

In this section, we present a brief description of P1's and P2's security against collective attacks and the main results of secure key rate. Here, we focus on collective attacks where Eve adopts the same attack to each system of Alice and Bob. For the first QKD protocol, P1, only signals originated from single-photon pulses emitted by both Alice and Bob are guaranteed to be secure while Eve's information is restricted by the Holevo bound [4, 10]. Since the WCPs' phase randomization makes the emitted quantum states of Alice and Bob into a classical mixture of states, it enables Alice and Bob to tag each pulse in principle though they do not need to do so in practice [28]. It is assumed that Eve competely knows the information from the multiphoton components (tagged portion). Then the information of Eve is composed of two portions, namely tagged and untagged portion, which can be written as (see Appendix A for more details)

$$\begin{aligned}\chi_1(A_1 : E) &= \chi_1^{\text{tag}}(A_1 : E) + \chi_1^{\text{untag}}(A_1 : E) \\ &= (Q_{\mu\nu}^Z - Q_{11}^Z) + Q_{11}^Z H\left(e_{11}^{BZ} + \frac{S_{11}}{2\sqrt{2}}\right).\end{aligned}\quad (1)$$

The mutual information between Alice and Bob, considering that the error-correction will leak extra information, is given by

$$I_1(A_1 : B_0) = Q_{\mu\nu}^Z - Q_{\mu\nu}^Z fH(E_{\mu\nu}^Z). \quad (2)$$

The secure key rate of P1 (per joint signal state emitted by Alice and Bob simultaneously in σ_z basis) can be written as

$$\begin{aligned}R_1 &= I_1(A_1 : B_0) - \chi_1(A_1 : E) \\ &= Q_{11}^Z \left[1 - H\left(e_{11}^{BZ} + \frac{S_{11}}{2\sqrt{2}}\right)\right] - Q_{\mu\nu}^Z fH(E_{\mu\nu}^Z),\end{aligned}\quad (3)$$

where $Q_{\mu\nu}^Z$ and $E_{\mu\nu}^Z$, the overall gain and quantum bit error rate (QBER), can be directly obtained from the experimental results. The subscript $\mu\nu$ means that Alice and Bob send out WCPs with intensity μ and ν , respectively. For the single-photon states, the gain Q_{11}^Z , bit error rate e_{11}^{BZ} and the Bell value S_{11} can be estimated by the decoy-state method. Here, the parameter f is the error correction efficiency (we take the value $f = 1.16$ in our simulation), and $H(e) = -e \log_2(e) - (1-e) \log_2(1-e)$ is the binary Shannon entropy function.

For QKD protocol P2, the multiphoton components are tagged whose information will be fully leaked to Eve [28]. Only signals originated from single-photon pulses emitted by both Alice and Bob are the untagged portion which can be extracted as secure keys. For the untagged portion, we use the min-entropy to bound Eve's knowledge of the secure keys, which has been applied to analyze security in Refs. [11, 27]. Details of this part can be found in Appendix B. The secure key rate of P2 is given

by

$$\begin{aligned}R_2 &= I_2(A_1 : B_0) - \chi_2(A_1 : E) \\ &= Q_{11}^Z \left[1 - \log_2 \left(1 + \sqrt{2 - \frac{S_{11}^2}{4}}\right)\right] - Q_{\mu\nu}^Z fH(E_{\mu\nu}^Z).\end{aligned}\quad (4)$$

The second term $Q_{\mu\nu}^Z fH(E_{\mu\nu}^Z)$ quantifies the amount of information needed for the error-correction. The non-trivial part of our bound is $\log_2 \left(1 + \sqrt{2 - \frac{S_{11}^2}{4}}\right) Q_{11}^Z$, which quantifies Eve's information.

When the phases of the WCPs sent by Alice and Bob are fully randomized, the density matrix of the quantum states should be written as

$$\rho = \int_0^{2\pi} \frac{d\theta}{2\pi} |\sqrt{\mu}e^{i\theta}\rangle \langle \sqrt{\mu}e^{i\theta}| = e^{-\mu} \sum_{n=0}^{\infty} \frac{\mu^n}{n!} |n\rangle \langle n|, \quad (5)$$

where θ and μ are the phase and intensity of the coherent states, respectively. Then the quantum channel can be considered as a photon number channel [20]. The overall gain and QBER in σ_z basis can be given by

$$\begin{aligned}Q_{\mu\nu}^Z &= Q_{\mu\nu}^{CZ} + Q_{\mu\nu}^{EZ} = \sum_{n=0}^{\infty} \sum_{m=0}^{\infty} \frac{\mu^n \nu^m}{n!m!} e^{-\mu-\nu} Y_{nm}^Z, \\ E_{\mu\nu}^Z Q_{\mu\nu}^Z &= e_d Q_{\mu\nu}^{CZ} + (1 - e_d) Q_{\mu\nu}^{EZ} \\ &= \sum_{n=0}^{\infty} \sum_{m=0}^{\infty} \frac{\mu^n \nu^m}{n!m!} e^{-\mu-\nu} e_{nm}^{BZ} Y_{nm}^Z,\end{aligned}\quad (6)$$

where Y_{nm}^Z (e_{nm}^{BZ}) is the yield (bit error rate), given that Alice and Bob send out n -photon and m -photon pulse, respectively. $Q_{\mu\nu}^{CZ}$ ($Q_{\mu\nu}^{EZ}$) is the total gain of a successful BSM when the polarization of the pulses sent by Alice and Bob are different (the same) in σ_z basis, which represents a correct (false) measurement result. e_d represents the overall misalignment-error probability of the system. The Bell value S_{11} is given by

$$\begin{aligned}S_{11} &= \frac{1}{2}(S_{11}^{\psi^-} + S_{11}^{\psi^+}) = S_{11}^{\psi^-}, \\ S_{11}^{\psi^-} &= \langle A_2 B_2 \rangle_{11}^{\psi^-} - \langle A_2 B_1 \rangle_{11}^{\psi^-} - \langle A_1 B_2 \rangle_{11}^{\psi^-} - \langle A_1 B_1 \rangle_{11}^{\psi^-},\end{aligned}\quad (7)$$

where we use $S_{11}^{\psi^-} = S_{11}^{\psi^+}$ because of symmetry. In our simulation, the expectation of single-photon states $\langle A_k \otimes B_l \rangle_{11}^{\psi^-} = \langle A_k B_l \rangle_{11}^{\psi^-}$ results from the successful projection into the Bell state $|\psi^-\rangle$ with appropriate setting of A_k and B_l , where $k, l \in \{1, 2\}$. So the expectation is given by

$$\begin{aligned}\langle A_k B_l \rangle_{11}^{\psi^-} &= (1 - 2e_d) \\ &\times \frac{Y_{H_{A_k} H_{B_l}}^{11\psi^-} + Y_{V_{A_k} V_{B_l}}^{11\psi^-} - Y_{H_{A_k} V_{B_l}}^{11\psi^-} - Y_{V_{A_k} H_{B_l}}^{11\psi^-}}{Y_{H_{A_k} H_{B_l}}^{11\psi^-} + Y_{V_{A_k} V_{B_l}}^{11\psi^-} + Y_{H_{A_k} V_{B_l}}^{11\psi^-} + Y_{V_{A_k} H_{B_l}}^{11\psi^-}},\end{aligned}\quad (8)$$

where $Y_{H_{A_k} V_{B_l}}^{11\psi^-}$ is a yield. The superscript $11\psi^-$ represents that Charlie obtains a Bell state $|\psi^-\rangle$ successfully,

given that both Alice and Bob send out single-photon states. The subscript $H_{A_k} V_{B_l}$ represents the joint quantum state that Alice sends out a positive eigenvalue corresponding to the eigenstate of setting A_k while Bob sends out a negative eigenvalue corresponding to the eigenstate of setting B_l .

We present two methods to obtain Y_{11}^Z , e_{11}^{BZ} and S_{11} , the relevant parameters which are needed to evaluate the key rate formula above, given that Alice and Bob send Charlie a finite number of signals and use a finite number of decoy states. We use the standard error analysis method [29, 30] to solve this problem (a rigorous estimation can be acquired by using large deviation theory, i.e., the Chernoff bound [31]). More precisely, we combine linear programming and analytical method, respectively, with two decoy states, to estimate all the lower bounds of Y_{11}^Z , e_{11}^{BZ} and S_{11} within single-photon states. Importantly, our methods are valid for arbitrary photon-number distribution of signals sent by Alice and Bob. To get more details of this part, please see Appendix C.

V. SIMULATION RESULTS

In this section, we analyze the behavior of the secret key rates of P1 and P2 provided in Eq. (3) and Eq. (4), respectively. In our simulation, the loss of fiber-based channel is 0.2 dB/km. For simplicity, we assume that all detectors are identical (i.e., they have the same detection efficiency and background count rate), and their background count rate, to a good approximation, is independent of incoming signals. We assume that the detection efficiency of Charlie is 40% and the background count rate is 3×10^{-6} . We use an intrinsic error rate that represents the misalignment and instability of the optical system. Furthermore, the security bound is fixed to be $\epsilon = 10^{-10}$.

The secure key rates of P1 and P2 in the asymptotic case are shown in Fig. 2 with blue dashed curve and black dashed curve, respectively. Meanwhile, we also present the simulation result of the MDI-QKD [16] with the red solid curve. We can see clearly that the secure key rate and secure distance of P1 are the same as MDI-QKD's in the asymptotic case. The reason lies in that the security proof based on entanglement distillation purification is equivalent to direct information-theoretic arguments with one-way classical communications. The secure key rate and secure distance of P2 are both less than P1's, since P2 requires fewer security assumptions, i.e., we do not require that Alice and Bob perfectly characterize their encoded quantum states.

In practice, we need to consider a finite number of decoy states. The simulation results using linear programming and analytical method with vacuum+decoy states in asymptotic-data case (finite-data case) are shown in Fig. 3 (Fig. 4). Notice that the key rates using the analytical method almost overlap with the one using linear programming in Fig. 3 and Fig. 4. In the asymptotic-

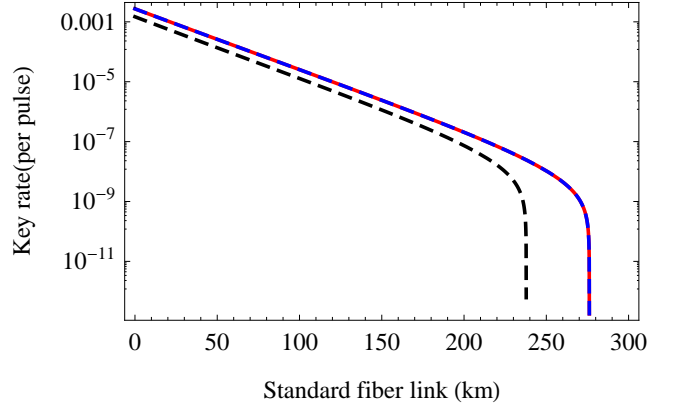


FIG. 2: (Color online) The secure key rates in asymptotic case. Asymptotic case means that Alice and Bob use infinite number of decoy states and send Charlie infinite data signals. We use the following practical experimental parameters: the detection efficiency η_d of Charlie is 40%, the intrinsic loss coefficient β of the standard telecom fiber channel is 0.2 dB/km, the overall misalignment-error probability e_d of the system is 1.5%, the background count rate p_d is 3×10^{-6} , the intensity of signal state μ is 0.3.

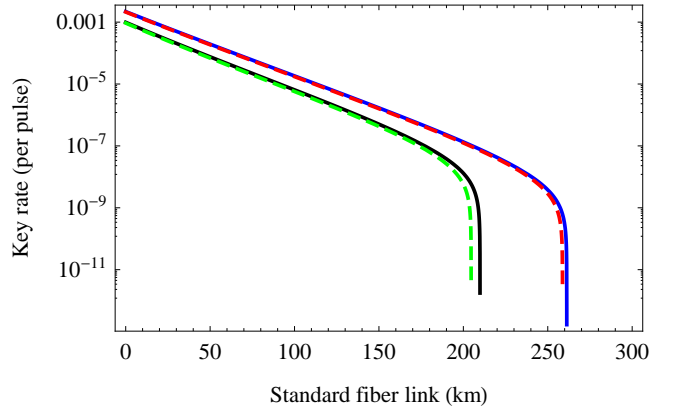


FIG. 3: (Color online) The secure key rates with two decoy states in asymptotic-data case. The intensities of signal state μ and one decoy state ν are 0.3 and 0.01, respectively, while the other decoy state is a vacuum state. We emphasize that the key rates with analytical method of Appendix C almost overlap with the one with linear programming, which shows that the analytical method provides an excellent estimation. The estimation using two decoy states gives a secure key rate which is nearly the same as the one using infinite decoy states. Therefore, two decoy states (vacuum+decoy) are enough for a near-optimal estimation, no matter how many decoy states are added, the secure key rate cannot be improved too much. In the asymptotic-data and two decoy states case, the security distances of P1 and P2 are more than 200 km.

data case (Fig. 3), the blue (black) solid curve represents the secure key rate of P1 (P2) under linear programming, while the red (green) dashed curve represents the secure key rate of P1 (P2) under analytical method. Comparing Fig. 2 with Fig. 3, we can see clearly that the key rates with two decoy states (vacuum+decoy) are close to the

corresponding ones with infinite number of decoy states. In finite-data case (Fig. 4), the statistical fluctuations are

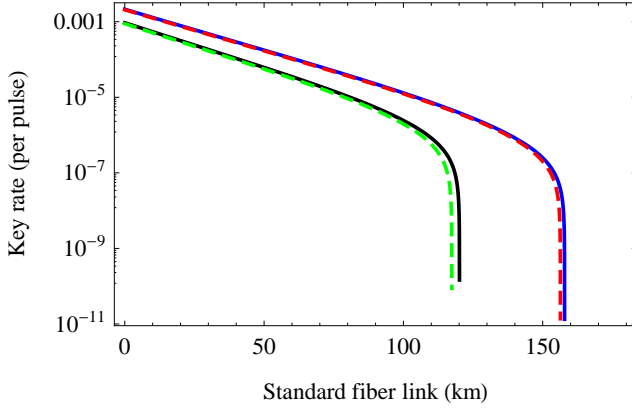


FIG. 4: (Color online) The secure key rates with statistical fluctuations. The intensities of signal state μ and one decoy state ν are 0.3 and 0.01, respectively, while the other decoy state is a vacuum state. The finite data is $N = 10^{14}$, the secure bound is $\epsilon = 10^{-10}$. In the finite-data and two decoy states case, the security distance of P1 is more than 150 km, and the security distance of P2 is more than 110 km.

simulated using the standard error analysis method [29]. For simplicity, we assume that Alice and Bob send same number of pulses for all $\mu_{A_k} \uplus \nu_{B_l}$ channels, denoted by N (an efficient parameter optimization method can be found in [32]). Here $\mu_{A_k} \uplus \nu_{B_l}$ is defined as the case that Alice sends out WCPs of intensity μ with setting A_k while Bob sends out WCPs of intensity ν with setting B_l , where $k \in \{0, 1\}$, $l \in \{0, 1, 2\}$. In the finite-data and two decoy states cases, the security distance of P1 (P2) is more than 150 km (110 km).

VI. CONCLUSION

In summary, we have proposed two QKD protocols, P1 and P2, inspired by E91 and MDI-QKD protocols. As to P1, the security assumptions and the secure key rate in asymptotic case are the same as MDI-QKD's. More importantly, in the security proof of P2, Alice and Bob's perfectly characterizing encoded quantum states is not required. Thus, P2 is more resistant to source-side attacks compared with MDI-QKD. The simulation results show that P2 is more practical using conventional laser sources and decoy-state method instead of the single-photon sources. P2 depends less on device but keeps a high secure key rate and long transmission distance. Moreover, the Bell value can be estimated accurately with conventional laser sources and finite-number decoy states method. We believe that this technique can be used in other fields of quantum information processing. The full parameter optimization of P1 and P2 needs to be done in the future.

VII. ACKNOWLEDGMENTS

This work was supported by the NNSF of China under Grant No. 61125502, the National Fundamental Research Program under Grant No. 2011CB921300, the CAS and the National High Technology Research and Development Program of China.

Appendix A: HOLEVO BOUND

Without loss of generality, the BB84 protocol implies that one can compute the bound by restricting consideration to collective attacks [4]. Considering the collective attacks, the final density matrix of Alice and Bob's joint quantum state can be given by

$$\rho_{AB} = \lambda_1 |\phi^+\rangle\langle\phi^+| + \lambda_2 |\phi^-\rangle\langle\phi^-| + \lambda_3 |\psi^+\rangle\langle\psi^+| + \lambda_4 |\psi^-\rangle\langle\psi^-|, \quad (\text{A1})$$

with $\sum_{i=1}^4 \lambda_i = 1$. The four Bell states

$$\begin{aligned} |\phi^+\rangle &= \frac{1}{\sqrt{2}}(|HH\rangle + |VV\rangle) = \frac{1}{\sqrt{2}}(|++\rangle + |--\rangle), \\ |\phi^-\rangle &= \frac{1}{\sqrt{2}}(|HH\rangle - |VV\rangle) = \frac{1}{\sqrt{2}}(|+-\rangle + |-+\rangle), \\ |\psi^+\rangle &= \frac{1}{\sqrt{2}}(|HV\rangle + |VH\rangle) = \frac{1}{\sqrt{2}}(|++\rangle - |--\rangle), \\ |\psi^-\rangle &= \frac{1}{\sqrt{2}}(|HV\rangle - |VH\rangle) = \frac{1}{\sqrt{2}}(|+-\rangle - |-+\rangle), \end{aligned} \quad (\text{A2})$$

constitute a complete orthogonal basis in two-dimensional Hilbert space. $|\phi^\pm\rangle$ ($|\phi^+\rangle, |\psi^+\rangle$) are perfectly correlated in σ_z (σ_x) basis, while $|\psi^\pm\rangle$ ($|\phi^-\rangle, |\psi^-\rangle$) are perfectly anticorrelated. Therefore, the bit error rates in σ_z and σ_x basis are given by

$$e^{BZ} = \lambda_3 + \lambda_4, \quad e^{BX} = \lambda_2 + \lambda_4. \quad (\text{A3})$$

The phase error rates in the two bases are

$$e^{PZ} = \lambda_2 + \lambda_4 = e^{BX}, \quad e^{PX} = \lambda_3 + \lambda_4 = e^{BZ}. \quad (\text{A4})$$

The secure key rate of the entanglement distillation purification-based QKD using one-way classical communications is [33, 34]

$$R_{EDP} = 1 - H(e^{BZ}) - H(e^{PZ}) = 1 - H(e^{BZ}) - H(e^{BX}). \quad (\text{A5})$$

Here, we use Holevo bound to estimate Eve's information [35, 36],

$$\begin{aligned} \chi(A : E) &= S(\rho_E) - \frac{1}{2}S(\rho_{E|0}) - \frac{1}{2}S(\rho_{E|1}) \\ &= H(e^{BX}), \end{aligned} \quad (\text{A6})$$

and the secure key rate is

$$\begin{aligned} R_{Inf} &= I(A : B) - \chi(A : E) \\ &= 1 - H(e^{BZ}) - H(e^{BX}) = R_{EDP}. \end{aligned} \quad (\text{A7})$$

We can see that the security proof based on entanglement distillation purification is equivalent to direct information-theoretic arguments with one-way classical communications.

The Bell operator can be written as

$$B = A_1 \otimes B_1 + A_1 \otimes B_2 + A_2 \otimes B_1 - A_2 \otimes B_2 \\ = \sqrt{2}(\sigma_z \otimes \sigma_z + \sigma_x \otimes \sigma_x). \quad (\text{A8})$$

Thus, the Bell value is given by [10]

$$S = \text{Tr}(B\rho_{AB}) \\ = \sqrt{2}\text{Tr}((\sigma_z \otimes \sigma_z + \sigma_x \otimes \sigma_x)\rho_{AB}) \\ = 2\sqrt{2}(\lambda_1 - \lambda_4) \\ = 2\sqrt{2}(1 - e^{BZ} - e^{BX}). \quad (\text{A9})$$

Instead of using the bit error rate e^{BX} in σ_x basis, the parameter from which Eve's information is inferred is the average Bell value S and the bit error rate e^{BZ} in σ_z basis, i.e., $e^{BX} = 1 - e^{BZ} - S/2\sqrt{2}$.

Consider that Alice and Bob encode their bits in the polarization degrees of freedom of phase-randomized WCPs. The information of Eve with two portions [28], i.e., tagged and untagged portion, can be written as

$$\chi_1(A_1 : E) = \chi_1^{\text{tag}}(A_1 : E) + \chi_1^{\text{untag}}(A_1 : E) \\ = (Q_{\mu\nu}^Z - Q_{11}^Z) + Q_{11}^Z H\left(1 - e_{11}^{BZ} - \frac{S_{11}}{2\sqrt{2}}\right) \\ = (Q_{\mu\nu}^Z - Q_{11}^Z) + Q_{11}^Z H\left(e_{11}^{BZ} + \frac{S_{11}}{2\sqrt{2}}\right), \quad (\text{A10})$$

where the superscripts *tag* and *untag* represent tagged portion and untagged portion, respectively. The mutual information between Alice and Bob, considering that the error-correction will leak extra information, is given by

$$I_1(A_1 : B_0) = Q_{\mu\nu}^Z - Q_{\mu\nu}^Z fH(E_{\mu\nu}^Z). \quad (\text{A11})$$

Finally, the secure key rate of P1 is given by

$$R_1 = I_1(A_1 : B_0) - \chi_1(A_1 : E) \\ = Q_{11}^Z \left[1 - H\left(e_{11}^{BZ} + \frac{S_{11}}{2\sqrt{2}}\right)\right] - Q_{\mu\nu}^Z fH(E_{\mu\nu}^Z). \quad (\text{A12})$$

Appendix B: MIN-ENTROPY

In this part, the goal is to guarantee the security proof of P2 although removing the assumption that encoded quantum states need to be characterized perfectly. Obviously, the first five assumptions in section II are also required in the security proof of DI-QKD. The secure key rate of DI-QKD [11] is

$$R = H_{\min}^{\text{DI}}(A_1|E) - H_{\text{con}}^{\text{DI}}(A_1|B_0), \quad (\text{B1})$$

where

$$H_{\min}^{\text{DI}}(A_1|E) = -\log_2 P_{\text{guess}}(a), \quad (\text{B2}) \\ H_{\text{con}}^{\text{DI}}(A_1|B_0) = H(e^{BZ}).$$

In above equations, $H_{\min}^{\text{DI}}(A_1|E)$ is the (quantum) min-entropy, which will be used for restricting the knowledge of Eve. By employing privacy amplification, we are able to make Eve's information arbitrarily small. $H_{\text{con}}^{\text{DI}}(A_1|B_0)$ is the conditional Shannon entropy which quantifies the amount of information needed for error-correction. a is the output (eigenvalue) of setting $\{A_1, A_2\}$, and $P_{\text{guess}}(a)$ is the maximal guessing probability which is used for quantifying the degree of unpredictability of Alice's measurement output a . The following bound will hold in Bell's inequality [37]

$$P_{\text{guess}}(a) \leq \frac{1}{2} + \frac{1}{2}\sqrt{2 - \frac{S^2}{4}}. \quad (\text{B3})$$

In the DI-QKD scheme, the loophole-free Bell test can ensure QKD security against untrusted detectors and arbitrarily dimensional quantum systems. P2 can be regarded as the modified time-reversed E91 and it is naturally immune to all possible detection-side attacks. The quantum states of P2 are required to be prepared in the two-dimensional Hilbert space, because the security of high-dimensional quantum states will not be guaranteed (for example, the four-dimensional separable state will have the property of two-dimensional maximally entangled state in Ref. [10]). Therefore, we can use the measurement data to calculate the Bell value with the assumption that the Hilbert space of quantum state preparation is two-dimensional. We use the min-entropy to bound Eve's information with the untagged portion

$$\chi_2^{\text{untag}}(A_1 : E) = Q_{11}^Z [1 - H_{\min}^{2\text{dim}}(A_1|E)] \\ \leq Q_{11}^Z \left[1 + \log_2 \left(\frac{1}{2} + \frac{1}{2}\sqrt{2 - \frac{S_{11}^2}{4}}\right)\right], \quad (\text{B4})$$

where the superscript 2 dim represents that the Hilbert space of quantum systems is two-dimensional. From the analysis above, it is not necessarily required that Alice and Bob perfectly characterize their encoded quantum states. Eve will acquire more information because the dimension of DI-QKD's quantum systems is arbitrary. Then the following inequality will hold,

$$H_{\min}^{2\text{dim}}(A_1|E) \geq H_{\min}^{\text{DI}}(A_1|E). \quad (\text{B5})$$

The secure key rate of P2 is given by

$$\begin{aligned}
R_2 &= I_2(A_1 : B_0) - \chi_2(A_1 : E) \\
&= I_2(A_1 : B_0) - [\chi_2^{\text{tag}}(A_1 : E) + \chi_2^{\text{untag}}(A_1 : E)] \\
&\geq Q_{\mu\nu}^Z - Q_{\mu\nu}^Z fH(E_{\mu\nu}^Z) - (Q_{\mu\nu}^Z - Q_{11}^Z) \\
&\quad - Q_{11}^Z \left[1 + \log_2 \left(\frac{1}{2} + \frac{1}{2} \sqrt{2 - \frac{S_{11}^2}{4}} \right) \right] \\
&= Q_{11}^Z \left[1 - \log_2 \left(1 + \sqrt{2 - \frac{S_{11}^2}{4}} \right) \right] - Q_{\mu\nu}^Z fH(E_{\mu\nu}^Z).
\end{aligned} \tag{B6}$$

Appendix C: ESTIMATE Q_{11}^Z , e_{11}^{BZ} and S_{11}

1. gain and error

Now, we evaluate the overall gain and QBER. Alice and Bob prepare phase-randomized WCPs with intensity μ_i and ν_j , respectively. The overall gain and QBER in σ_z basis (Alice chooses setting A_1 and Bob chooses setting B_0) can be written as [30]

$$\begin{aligned}
Q_{\mu_i\nu_j}^Z &= Q_{\mu_i\nu_j}^{CZ} + Q_{\mu_i\nu_j}^{EZ} = \sum_{n=0}^{\infty} \sum_{m=0}^{\infty} \frac{\mu_i^n \nu_j^m}{n!m!} e^{-\mu_i - \nu_j} Y_{nm}^Z, \\
E_{\mu_i\nu_j}^Z Q_{\mu_i\nu_j}^Z &= e_d Q_{\mu_i\nu_j}^{CZ} + (1 - e_d) Q_{\mu_i\nu_j}^{EZ} \\
&= \sum_{n=0}^{\infty} \sum_{m=0}^{\infty} \frac{\mu_i^n \nu_j^m}{n!m!} e^{-\mu_i - \nu_j} e_{nm}^{BZ} Y_{nm}^Z,
\end{aligned} \tag{C1}$$

where

$$\begin{aligned}
Q_{\mu_i\nu_j}^{CZ} &= 2(1 - p_d)^2 e^{-\frac{\omega}{2}} \left[1 - (1 - p_d) e^{-\frac{\mu_i \eta_a}{2}} \right] \\
&\quad \times \left[1 - (1 - p_d) e^{-\frac{\nu_j \eta_b}{2}} \right], \\
Q_{\mu_i\nu_j}^{EZ} &= 2p_d(1 - p_d)^2 e^{-\frac{\omega}{2}} \left[I_0(2x) - (1 - p_d) e^{-\frac{\omega}{2}} \right].
\end{aligned} \tag{C2}$$

In the above equations, p_d is the background count rate, $I_0(2x)$ is the modified Bessel function of the first kind, e_d represents the misalignment-error probability, and $\omega = \mu_i \eta_a + \nu_j \eta_b$, $x = \frac{\sqrt{\mu_i \nu_j \eta_a \eta_b}}{2}$. $\eta_a = \eta_b = \eta_d \times 10^{-\beta L/20}$ is the total efficiency including channel transmittance efficiency $10^{-\beta L/20}$ and detection efficiency η_d . Considering the symmetric scenario, the distance between Alice (Bob) and Charlie is $L/2$.

Now, we focus on the joint quantum state. Alice sends out a positive eigenvalue corresponding to the eigenstate $|H_{A_1}\rangle = |H\rangle$ of setting A_1 and Bob sends out a positive eigenvalue corresponding to the eigenstate $|H_{B_1}\rangle = \cos \frac{\pi}{8} |H\rangle + \cos \frac{3\pi}{8} |V\rangle$ of setting B_1 , i.e.,

$$\begin{aligned}
|H_{A_1}\rangle \otimes |H_{B_1}\rangle &= |e^{i\phi_a} \sqrt{\mu_i \eta_a}\rangle_H \otimes \left(\cos \frac{\pi}{8} |e^{i\phi_b} \sqrt{\nu_j \eta_b}\rangle_H \right. \\
&\quad \left. + \cos \frac{3\pi}{8} |e^{i\phi_b} \sqrt{\nu_j \eta_b}\rangle_V \right),
\end{aligned} \tag{C3}$$

where ϕ_a and ϕ_b are the overall randomized phases, while $|H\rangle$ ($|V\rangle$) is a positive (negative) eigenvalue corresponding to the eigenstate of σ_z basis. Then the quantum state passing through the beam splitter and four polarization beam splitters is given by

$$\begin{aligned}
&\left| e^{i\phi_a} \sqrt{\frac{\mu_i \eta_a}{2}} + \cos \frac{\pi}{8} e^{i\phi_b} \sqrt{\frac{\nu_j \eta_b}{2}} \right\rangle_{1H} \left| \cos \frac{3\pi}{8} e^{i\phi_b} \sqrt{\frac{\nu_j \eta_b}{2}} \right\rangle_{1V} \\
&\otimes \left| e^{i\phi_a} \sqrt{\frac{\mu_i \eta_a}{2}} - \cos \frac{\pi}{8} e^{i\phi_b} \sqrt{\frac{\nu_j \eta_b}{2}} \right\rangle_{2H} \\
&\otimes \left| -\cos \frac{3\pi}{8} e^{i\phi_b} \sqrt{\frac{\nu_j \eta_b}{2}} \right\rangle_{2V},
\end{aligned} \tag{C4}$$

where the four detection modes are $1H$, $1V$, $2H$ and $2V$. Therefore, the detection probabilities for the four detectors are given by

$$\begin{aligned}
D_{1H} &= 1 - (1 - p_d) \exp(-|\frac{e^{i\phi_a} \sqrt{\mu_i \eta_a} + \cos \frac{\pi}{8} e^{i\phi_b} \sqrt{\nu_j \eta_b}}{\sqrt{2}}|^2), \\
D_{1V} &= 1 - (1 - p_d) \exp(-|\frac{\cos \frac{3\pi}{8} e^{i\phi_b} \sqrt{\nu_j \eta_b}}{\sqrt{2}}|^2), \\
D_{2H} &= 1 - (1 - p_d) \exp(-|\frac{e^{i\phi_a} \sqrt{\mu_i \eta_a} - \cos \frac{\pi}{8} e^{i\phi_b} \sqrt{\nu_j \eta_b}}{\sqrt{2}}|^2), \\
D_{2V} &= 1 - (1 - p_d) \exp(-|\frac{-\cos \frac{3\pi}{8} e^{i\phi_b} \sqrt{\nu_j \eta_b}}{\sqrt{2}}|^2).
\end{aligned} \tag{C5}$$

The gain $Q_{H_{A_1} H_{B_1}}^{\mu_i \nu_j \psi^-}$ is defined as the probability that Alice sends out a positive eigenvalue corresponding to the eigenstate $|H_{A_1}\rangle = |H\rangle$ of setting A_1 with the intensity μ_i , while Bob sends out a positive eigenvalue corresponding to the eigenstate $|H_{B_1}\rangle = \cos \frac{\pi}{8} |H\rangle + \cos \frac{3\pi}{8} |V\rangle$ of setting B_1 with the intensity ν_j . Meanwhile, Charlie has a successful Bell state $|\psi^-\rangle$ measurement event. Therefore,

$$\begin{aligned}
Q_{H_{A_1} H_{B_1}}^{\mu_i \nu_j \psi^-} &= \frac{1}{2\pi} \int_0^{2\pi} \frac{1}{4} [D_{1H} D_{2V} (1 - D_{2H}) (1 - D_{1V}) \\
&\quad + D_{2H} D_{1V} (1 - D_{1H}) (1 - D_{2V})] d\phi,
\end{aligned} \tag{C6}$$

where $Q_{H_{A_1} H_{B_1}}^{\mu_i \nu_j \psi^-}$ is averaged over random phases ϕ_a and ϕ_b , $\phi = \phi_a - \phi_b$. By substituting Eq. (C5) into Eq. (C6), we have

$$\begin{aligned}
Q_{H_{A_1} H_{B_1}}^{\mu_i \nu_j \psi^-} &= \sum_{n=0}^{\infty} \sum_{m=0}^{\infty} \frac{\mu_i^n \nu_j^m}{n!m!} e^{-\mu_i - \nu_j} Y_{nm}^{\psi^-} \\
&= \frac{1}{2} (1 - p_d)^2 e^{-\frac{\omega}{2}} I_0(2x \cos \frac{\pi}{8}) + \frac{1}{2} (1 - p_d)^4 e^{-\omega} \\
&\quad - \frac{1}{2} (1 - p_d)^3 e^{-\frac{2\mu_i \eta_a + (1 + \cos^2 \frac{\pi}{8}) \nu_j \eta_b}{2}} \\
&\quad - \frac{1}{2} (1 - p_d)^3 e^{-\frac{\mu_i \eta_a + (1 + \cos^2 \frac{3\pi}{8}) \nu_j \eta_b}{2}} I_0(2x \cos \frac{\pi}{8}).
\end{aligned} \tag{C7}$$

According to the above procedures, we can also obtain

$$\begin{aligned}
Q_{H_{A_1} V_{B_1}}^{\mu_i \nu_j \psi^-} &= \sum_{n=0}^{\infty} \sum_{m=0}^{\infty} \frac{\mu_i^n \nu_j^m}{n!m!} e^{-\mu_i - \nu_j} Y_{H_{A_1} V_{B_1}}^{nm\psi^-} \\
&= \frac{1}{2}(1-p_d)^2 e^{-\frac{\omega}{2}} I_0(2x \cos \frac{3\pi}{8}) + \frac{1}{2}(1-p_d)^4 e^{-\omega} \\
&\quad - \frac{1}{2}(1-p_d)^3 e^{-\frac{2\mu_i \eta_a + (1+\cos^2 \frac{3\pi}{8})\nu_j \eta_b}{2}} \\
&\quad - \frac{1}{2}(1-p_d)^3 e^{-\frac{\mu_i \eta_a + (1+\cos^2 \frac{\pi}{8})\nu_j \eta_b}{2}} I_0(2x \cos \frac{3\pi}{8}), \tag{C8}
\end{aligned}$$

$$\begin{aligned}
Q_{H_{A_2} H_{B_1}}^{\mu_i \nu_j \psi^-} &= \sum_{n=0}^{\infty} \sum_{m=0}^{\infty} \frac{\mu_i^n \nu_j^m}{n!m!} e^{-\mu_i - \nu_j} Y_{H_{A_2} H_{B_1}}^{nm\psi^-} \\
&= \frac{1}{2}(1-p_d)^2 e^{-\frac{\omega}{2}} I_0(\sqrt{2}x(\cos \frac{\pi}{8} - \cos \frac{3\pi}{8})) \\
&\quad - \frac{1}{2}(1-p_d)^3 e^{-\frac{\frac{3}{2}\mu_i \eta_a + (1+\cos^2 \frac{\pi}{8})\nu_j \eta_b}{2}} I_0(\sqrt{2}x \cos \frac{3\pi}{8}) \\
&\quad - \frac{1}{2}(1-p_d)^3 e^{-\frac{\frac{3}{2}\mu_i \eta_a + (1+\cos^2 \frac{3\pi}{8})\nu_j \eta_b}{2}} I_0(\sqrt{2}x \cos \frac{\pi}{8}) \\
&\quad + \frac{1}{2}(1-p_d)^4 e^{-\omega}, \tag{C9}
\end{aligned}$$

$$\begin{aligned}
Q_{H_{A_2} V_{B_1}}^{\mu_i \nu_j \psi^-} &= \sum_{n=0}^{\infty} \sum_{m=0}^{\infty} \frac{\mu_i^n \nu_j^m}{n!m!} e^{-\mu_i - \nu_j} Y_{H_{A_2} V_{B_1}}^{nm\psi^-} \\
&= \frac{1}{2}(1-p_d)^2 e^{-\frac{\omega}{2}} I_0(\sqrt{2}x(\cos \frac{\pi}{8} + \cos \frac{3\pi}{8})) \\
&\quad - \frac{1}{2}(1-p_d)^3 e^{-\frac{\frac{3}{2}\mu_i \eta_a + (1+\cos^2 \frac{\pi}{8})\nu_j \eta_b}{2}} I_0(\sqrt{2}x \cos \frac{3\pi}{8}) \\
&\quad - \frac{1}{2}(1-p_d)^3 e^{-\frac{\frac{3}{2}\mu_i \eta_a + (1+\cos^2 \frac{3\pi}{8})\nu_j \eta_b}{2}} I_0(\sqrt{2}x \cos \frac{\pi}{8}) \\
&\quad + \frac{1}{2}(1-p_d)^4 e^{-\omega}, \tag{C10}
\end{aligned}$$

and

$$\begin{aligned}
Q_{H_{A_1} H_{B_1}}^{\mu_i \nu_j \psi^-} &= Q_{V_{A_1} V_{B_1}}^{\mu_i \nu_j \psi^-} = Q_{H_{A_1} V_{B_2}}^{\mu_i \nu_j \psi^-} = Q_{V_{A_1} H_{B_2}}^{\mu_i \nu_j \psi^-}, \\
Q_{H_{A_1} V_{B_1}}^{\mu_i \nu_j \psi^-} &= Q_{V_{A_1} H_{B_1}}^{\mu_i \nu_j \psi^-} = Q_{H_{A_1} V_{B_2}}^{\mu_i \nu_j \psi^-} = Q_{V_{A_1} H_{B_2}}^{\mu_i \nu_j \psi^-}, \tag{C11} \\
Q_{H_{A_2} H_{B_1}}^{\mu_i \nu_j \psi^-} &= Q_{V_{A_2} V_{B_1}}^{\mu_i \nu_j \psi^-} = Q_{H_{A_2} V_{B_2}}^{\mu_i \nu_j \psi^-} = Q_{V_{A_2} H_{B_2}}^{\mu_i \nu_j \psi^-}, \\
Q_{H_{A_2} V_{B_1}}^{\mu_i \nu_j \psi^-} &= Q_{V_{A_2} H_{B_1}}^{\mu_i \nu_j \psi^-} = Q_{H_{A_2} H_{B_2}}^{\mu_i \nu_j \psi^-} = Q_{V_{A_2} V_{B_2}}^{\mu_i \nu_j \psi^-}.
\end{aligned}$$

2. Asymptotic case

The gain of single-photon states (untagged portion) in σ_z basis, Q_{11}^Z , is given by

$$Q_{11}^Z = \mu \nu e^{-\mu - \nu} Y_{11}^Z. \tag{C12}$$

For the asymptotic case (with infinite number of decoy states and infinite data length), the yield and bit error

rate in σ_z basis with single-photon states are given by [30]

$$\begin{aligned}
Y_{11}^Z &= (1-p_d)^2 \left[\frac{\eta_a \eta_b}{2} + (2\eta_a + 2\eta_b - 3\eta_a \eta_b) p_d \right. \\
&\quad \left. + 4(1-\eta_a)(1-\eta_b) p_d^2 \right], \\
e_{11}^{BZ} Y_{11}^Z &= e_0 Y_{11}^Z - (e_0 - e_d)(1-p_d)^2(1-2p_d) \frac{\eta_a \eta_b}{2}, \tag{C13}
\end{aligned}$$

where $e_0 = \frac{1}{2}$. The Bell value $S_{11}^{\psi^-}$ of single-photon states is given by

$$S_{11}^{\psi^-} = \langle A_2 B_2 \rangle_{11}^{\psi^-} - \langle A_2 B_1 \rangle_{11}^{\psi^-} - \langle A_1 B_2 \rangle_{11}^{\psi^-} - \langle A_1 B_1 \rangle_{11}^{\psi^-}, \tag{C14}$$

where

$$\begin{aligned}
\langle A_k B_l \rangle_{11}^{\psi^-} &= (1 - 2e_d) \\
&\quad \times \frac{Y_{H_{A_k} H_{B_l}}^{11\psi^-} + Y_{V_{A_k} V_{B_l}}^{11\psi^-} - Y_{H_{A_k} V_{B_l}}^{11\psi^-} - Y_{V_{A_k} H_{B_l}}^{11\psi^-}}{Y_{H_{A_k} H_{B_l}}^{11\psi^-} + Y_{V_{A_k} H_{B_l}}^{11\psi^-} + Y_{H_{A_k} V_{B_l}}^{11\psi^-} + Y_{V_{A_k} V_{B_l}}^{11\psi^-}}, \tag{C15}
\end{aligned}$$

$k, l \in \{1, 2\}$. Thereinto,

$$\begin{aligned}
Y_{H_{A_1} H_{B_1}}^{11\psi^-} &= \cos^2 \frac{\pi}{8} \frac{p_d}{4} (1-p_d)^2 [1 - (1-2p_d)(1-\eta_a) \\
&\quad \times (1-\eta_b)] + \frac{p_d}{8} \cos^2 \frac{3\pi}{8} (1-p_d)^2 \\
&\quad \times [(2-\eta_a-\eta_b) + 2(1-p_d)(1-\eta_a)(1-\eta_b)] \\
&\quad + \frac{(1-p_d)^2}{8} \cos^2 \frac{3\pi}{8} [p_d(\eta_a + \eta_b) \\
&\quad + (1-2p_d)\eta_a \eta_b + 2p_d^2(1-\eta_a)(1-\eta_b)], \tag{C16}
\end{aligned}$$

$$\begin{aligned}
Y_{H_{A_1} V_{B_1}}^{11\psi^-} &= \cos^2 \frac{3\pi}{8} \frac{p_d}{4} (1-p_d)^2 [1 - (1-2p_d)(1-\eta_a) \\
&\quad \times (1-\eta_b)] + \frac{p_d}{8} \cos^2 \frac{\pi}{8} (1-p_d)^2 \\
&\quad \times [(2-\eta_a-\eta_b) + 2(1-p_d)(1-\eta_a)(1-\eta_b)] \\
&\quad + \frac{(1-p_d)^2}{8} \cos^2 \frac{\pi}{8} [p_d(\eta_a + \eta_b) \\
&\quad + (1-2p_d)\eta_a \eta_b + 2p_d^2(1-\eta_a)(1-\eta_b)], \tag{C17}
\end{aligned}$$

$$\begin{aligned}
Y_{H_{A_2} H_{B_1}}^{11\psi^-} &= \frac{p_d}{8} (1-p_d)^2 [1 - (1-2p_d)(1-\eta_a)(1-\eta_b)] \\
&\quad + \frac{p_d}{8} (\cos \frac{\pi}{8} + \cos \frac{3\pi}{8})^2 (1-p_d)^2 [(2-\eta_a-\eta_b) \\
&\quad + 2(1-p_d)(1-\eta_a)(1-\eta_b)] \\
&\quad + \frac{(1-p_d)^2}{16} (\cos \frac{\pi}{8} - \cos \frac{3\pi}{8})^2 [p_d(\eta_a + \eta_b) \\
&\quad + (1-2p_d)\eta_a \eta_b + 2p_d^2(1-\eta_a)(1-\eta_b)], \tag{C18}
\end{aligned}$$

$$\begin{aligned}
Y_{H_{A_2}V_{B_1}}^{11\psi^-} &= \frac{p_d}{8}(1-p_d)^2[1 - (1-2p_d)(1-\eta_a)(1-\eta_b)] \\
&+ \frac{p_d}{8}(\cos\frac{\pi}{8} - \cos\frac{3\pi}{8})^2(1-p_d)^2[(2-\eta_a-\eta_b) \\
&+ 2(1-p_d)(1-\eta_a)(1-\eta_b)] \\
&+ \frac{(1-p_d)^2}{16}(\cos\frac{\pi}{8} + \cos\frac{3\pi}{8})^2[p_d(\eta_a+\eta_b) \\
&+ (1-2p_d)\eta_a\eta_b + 2p_d^2(1-\eta_a)(1-\eta_b)], \tag{C19}
\end{aligned}$$

and

$$\begin{aligned}
Y_{H_{A_1}H_{B_1}}^{11\psi^-} &= Y_{V_{A_1}V_{B_1}}^{11\psi^-} = Y_{H_{A_1}H_{B_2}}^{11\psi^-} = Y_{V_{A_1}V_{B_2}}^{11\psi^-}, \\
Y_{H_{A_1}V_{B_1}}^{11\psi^-} &= Y_{V_{A_1}H_{B_1}}^{11\psi^-} = Y_{H_{A_1}V_{B_2}}^{11\psi^-} = Y_{V_{A_1}H_{B_2}}^{11\psi^-}, \\
Y_{H_{A_2}H_{B_1}}^{11\psi^-} &= Y_{V_{A_2}V_{B_1}}^{11\psi^-} = Y_{H_{A_2}V_{B_2}}^{11\psi^-} = Y_{V_{A_2}H_{B_2}}^{11\psi^-}, \\
Y_{H_{A_2}V_{B_1}}^{11\psi^-} &= Y_{V_{A_2}H_{B_1}}^{11\psi^-} = Y_{H_{A_2}H_{B_2}}^{11\psi^-} = Y_{V_{A_2}V_{B_2}}^{11\psi^-}. \tag{C20}
\end{aligned}$$

3. Finite decoy-state case

In practical demonstrations, the length of the raw key is finite, which will induce statistical fluctuations for the parameter estimation. Here, we consider the effect of finite length raw key based on standard error analysis method [29, 30]. The estimations of Y_{11}^Z , e_{11}^{BZ} and $S_{11}^{\psi^-}$ are constrained optimization problems, which are linear and can be efficiently solved by linear programming [30, 32].

Now, we consider an analytical estimation method with two decoy states [38], $\mu_2 = \nu_2 > \mu_1 = \nu_1 > \mu_0 = \nu_0 = 0$. The lower bound of Y_{11}^{ZL} , the upper bound of Y_{11}^{ZU} and the lower bound of e_{11}^{BZL} are given by

$$\begin{aligned}
Y_{11}^{ZL} &\geq \frac{1}{\mu_2^2\mu_1^2(\mu_2-\mu_1)} \left[\mu_2^3(e^{2\mu_1}Q_{\mu_1\mu_1}^Z + Q_{00}^Z \right. \\
&\quad \left. - e^{\mu_1}Q_{\mu_10}^Z - e^{\mu_1}Q_{0\mu_1}^Z) - \mu_1^3(e^{2\mu_2}Q_{\mu_2\mu_2}^Z \right. \\
&\quad \left. + Q_{00}^Z - e^{\mu_2}Q_{\mu_20}^Z - e^{\mu_2}Q_{0\mu_2}^Z) \right], \tag{C21}
\end{aligned}$$

$$Y_{11}^{ZU} \leq \frac{1}{\mu_1^2} [e^{2\mu_1}Q_{\mu_1\mu_1}^Z + Q_{00}^Z - e^{\mu_1}Q_{\mu_10}^Z - e^{\mu_1}Q_{0\mu_1}^Z], \tag{C22}$$

$$\begin{aligned}
e_{11}^{BZL} &\geq \frac{1}{\mu_2^2\mu_1^2(\mu_2-\mu_1)Y_{11}^{ZU}} \left\{ \mu_2^3 \left[e^{2\mu_1}E_{\mu_1\mu_1}^Z Q_{\mu_1\mu_1}^Z \right. \right. \\
&\quad \left. \left. + E_{00}^Z Q_{00}^Z - e^{\mu_1}E_{\mu_10}^Z Q_{\mu_10}^Z - e^{\mu_1}E_{0\mu_1}^Z Q_{0\mu_1}^Z \right] \right. \\
&\quad \left. - \mu_1^3 \left[e^{2\mu_2}E_{\mu_2\mu_2}^Z Q_{\mu_2\mu_2}^Z + E_{00}^Z Q_{00}^Z \right. \right. \\
&\quad \left. \left. - e^{\mu_2}E_{\mu_20}^Z Q_{\mu_20}^Z - e^{\mu_2}E_{0\mu_2}^Z Q_{0\mu_2}^Z \right] \right\}. \tag{C23}
\end{aligned}$$

Combining Eq. (C11) and Eq. (C20), we can use the following equations to estimate the lower bound of $S_{11}^{\psi^-}$,

$$\begin{aligned}
S_{11}^{\psi^-L} &\geq 2(1-2e_d) \\
&\times \left(\frac{Y_{H_{A_1}V_{B_1}}^{11\psi^-L} - Y_{H_{A_1}H_{B_1}}^{11\psi^-U}}{Y_{H_{A_1}H_{B_1}}^{11\psi^-U} + Y_{H_{A_1}V_{B_1}}^{11\psi^-U}} + \frac{Y_{H_{A_2}V_{B_1}}^{11\psi^-L} - Y_{H_{A_2}H_{B_1}}^{11\psi^-U}}{Y_{H_{A_2}H_{B_1}}^{11\psi^-U} + Y_{H_{A_2}V_{B_1}}^{11\psi^-U}} \right), \tag{C24}
\end{aligned}$$

where

$$\begin{aligned}
Y_{H_{A_k}V_{B_l}}^{11\psi^-L} &\geq \frac{1}{\mu_2^2\mu_1^2(\mu_2-\mu_1)} \left[\mu_2^3(e^{2\mu_1}Q_{H_{A_k}V_{B_l}}^{\mu_1\mu_1\psi^-} + Q_{H_{A_k}V_{B_l}}^{00\psi^-} \right. \\
&\quad \left. - e^{\mu_1}Q_{H_{A_k}V_{B_l}}^{\mu_10\psi^-} - e^{\mu_1}Q_{H_{A_k}V_{B_l}}^{0\mu_1\psi^-} \right) \\
&\quad \left. - \mu_1^3(e^{2\mu_2}Q_{H_{A_k}V_{B_l}}^{\mu_2\mu_2\psi^-} + Q_{H_{A_k}V_{B_l}}^{00\psi^-} \right. \\
&\quad \left. - e^{\mu_2}Q_{H_{A_k}V_{B_l}}^{\mu_20\psi^-} - e^{\mu_2}Q_{H_{A_k}V_{B_l}}^{0\mu_2\psi^-} \right], \tag{C25}
\end{aligned}$$

$$\begin{aligned}
Y_{H_{A_k}H_{B_l}}^{11\psi^-U} &\leq \frac{1}{\mu_1^2} \left[e^{2\mu_1}Q_{H_{A_k}H_{B_l}}^{\mu_1\mu_1\psi^-} + Q_{H_{A_k}H_{B_l}}^{00\psi^-} \right. \\
&\quad \left. - e^{\mu_1}Q_{H_{A_k}H_{B_l}}^{\mu_10\psi^-} - e^{\mu_1}Q_{H_{A_k}H_{B_l}}^{0\mu_1\psi^-} \right], \tag{C26}
\end{aligned}$$

$$\begin{aligned}
Y_{H_{A_k}V_{B_l}}^{11\psi^-U} &\leq \frac{1}{\mu_1^2} \left[e^{2\mu_1}Q_{H_{A_k}V_{B_l}}^{\mu_1\mu_1\psi^-} + Q_{H_{A_k}V_{B_l}}^{00\psi^-} \right. \\
&\quad \left. - e^{\mu_1}Q_{H_{A_k}V_{B_l}}^{\mu_10\psi^-} - e^{\mu_1}Q_{H_{A_k}V_{B_l}}^{0\mu_1\psi^-} \right], \tag{C27}
\end{aligned}$$

and $k, l \in \{1, 2\}$.

-
- [1] C. H. Bennett and G. Brassard, in *Proceedings of IEEE International Conference on Computers, Systems, and Signal Processing* (IEEE, New York, 1984), p. 175.
[2] A. K. Ekert, Phys. Rev. Lett. **67**, 661 (1991).
[3] N. Gisin, G. Ribordy, W. Tittel, and H. Zbinden, Rev. Mod. Phys. **74**, 145 (2002).
[4] V. Scarani, H. Bechmann-Pasquinucci, N. J. Cerf, M. Dušek, N. Lütkenhaus, and M. Peev, Rev. Mod. Phys. **81**, 1301 (2009).
[5] Y. Zhao, C.-H. F. Fung, B. Qi, C. Chen, and H.-K. Lo,

- Phys. Rev. A **78**, 042333 (2008).
[6] F. Xu, B. Qi, and H.-K. Lo, New J. Phys. **12**, 113026 (2010).
[7] L. Lydersen, C. Wiechers, C. Wittmann, D. Elser, J. Skaar, and V. Makarov, Nature Photon. **4**, 686 (2010).
[8] H. Weier, H. Krauss, M. Rau, M. Fürst, S. Nauerth, and H. Weinfurter, New J. Phys. **13**, 073024 (2011).
[9] I. Gerhardt, Q. Liu, A. Lamas-Linares, J. Skaar, C. Kurtz, and V. Makarov, Nature Commun. **2**, 349 (2011).
[10] S. Pironio, A. Acin, N. Brunner, N. Gisin, S. Massar, and

- V. Scarani, New J. Phys. **11**, 045021 (2009).
- [11] L. Masanes, S. Pironio, and A. Acín, Nature Commun. **2**, 238 (2011).
 - [12] C. C. W. Lim, C. Portmann, M. Tomamichel, R. Renner, and N. Gisin, Phys. Rev. X **3**, 031006 (2013).
 - [13] M. Giustina, A. Mech, S. Ramelow, B. Wittmann, J. Kofler, J. Beyer, A. Lita, B. Calkins, T. Gerrits, S. W. Nam, R. Ursin, and A. Zeilinger, Nature **497**, 227 (2013).
 - [14] B. G. Christensen, K. T. McCusker, J. B. Altepeter, B. Calkins, T. Gerrits, A. E. Lita, A. Miller, L. K. Shalm, Y. Zhang, S. W. Nam, N. Brunner, C. C. W. Lim, N. Gisin, and P. G. Kwiat, Phys. Rev. Lett. **111**, 130406 (2013).
 - [15] N. Gisin, S. Pironio, and N. Sangouard, Phys. Rev. Lett. **105**, 070501 (2010).
 - [16] H.-K. Lo, M. Curty, and B. Qi, Phys. Rev. Lett. **108**, 130503 (2012).
 - [17] E. Biham, B. Huttner, and T. Mor, Phys. Rev. A **54**, 2651 (1996).
 - [18] H. Inamori, Algorithmica **34**, 340 (2002).
 - [19] W.-Y. Hwang, Phys. Rev. Lett. **91**, 057901 (2003).
 - [20] H.-K. Lo, X. Ma, and K. Chen, Phys. Rev. Lett. **94**, 230504 (2005).
 - [21] X.-B. Wang, Phys. Rev. Lett. **94**, 230503 (2005).
 - [22] R. Ursin, F. Tiefenbacher, T. Schmitt-Manderbach, H. Weier, T. Scheidl, M. Lindenthal, B. Blauensteiner, T. Jennewein, J. Perdigues, P. Trojek, B. Ömer, M. Fürst, M. Meyenburg, J. Rarity, Z. Sodnik, C. Barbieri, H. Weinfurter, and A. Zeilinger, Nature Phys. **3**, 481 (2007).
 - [23] X. Ma, C.-H. F. Fung, and H.-K. Lo, Phys. Rev. A **76**, 012307 (2007).
 - [24] J. Barrett, R. Colbeck, and A. Kent, Phys. Rev. Lett. **110**, 010503 (2013).
 - [25] M. Pawłowski and N. Brunner, Phys. Rev. A **84**, 010302(R) (2011).
 - [26] Z.-Q. Yin, C.-H. F. Fung, X. Ma, C.-M. Zhang, H.-W. Li, W. Chen, S. Wang, G.-C. Guo, and Z.-F. Han, Phys. Rev. A **88**, 062322 (2013).
 - [27] H.-W. Li, Z.-Q. Yin, W. Chen, S. Wang, G.-C. Guo, and Z.-F. Han, Phys. Rev. A **89**, 032302 (2014).
 - [28] D. Gottesman, H.-K. Lo, N. Lütkenhaus, and J. Preskill, Quant. Inf. Comput. **4**, 325 (2004).
 - [29] X. Ma, B. Qi, Y. Zhao, and H.-K. Lo, Phys. Rev. A **72**, 012326 (2005).
 - [30] X. Ma, C.-H. F. Fung, and M. Razavi, Phys. Rev. A **86**, 052305 (2012).
 - [31] M. Curty, F. Xu, W. Cui, C. C. W. Lim, K. Tamaki, and H.-K. Lo, Nature Commun. **5**, 3732 (2014).
 - [32] F. Xu, H. Xu, and H.-K. Lo, Phys. Rev. A **89**, 052333 (2014).
 - [33] C. H. Bennett, D. P. DiVincenzo, J. A. Smolin, and W. K. Wootters, Phys. Rev. A **54**, 3824 (1996).
 - [34] P. W. Shor and J. Preskill, Phys. Rev. Lett. **85**, 441 (2000).
 - [35] B. Kraus, N. Gisin, and R. Renner, Phys. Rev. Lett. **95**, 080501 (2005).
 - [36] R. Renner, N. Gisin, and B. Kraus, Phys. Rev. A **72**, 012332 (2005).
 - [37] S. Pironio, A. Acín, S. Massar, A. Boyer de La Giroday, D. N. Matsukevich, P. Maunz, S. Olmschenk, D. Hayes, L. Luo, T. A. Manning, and C. Monroe, Nature **464**, 1021 (2010).
 - [38] F. Xu, M. Curty, B. Qi, and H.-K. Lo, New J. Phys. **15**, 113007 (2013).